

Fingerprints of superconducting stripes in hole-doped cuprates

Ivar Martin¹ and C. Panagopoulos^{2,3}

¹Theoretical Division, Los Alamos National Laboratory, Los Alamos, New Mexico 87545, USA

²Department of Physics, University of Crete and FORTH, 71003 Heraklion, Greece and

³Division of Physics and Applied Physics, School of Physical and Mathematical Sciences, Nanyang Technological University, 6373616 Singapore

(Dated: January 26, 2023)

One of the central mysteries of the high-temperature cuprate superconductors is the nature of the *pseudogap* regime (PG) that extends from the parent Mott insulator to at least optimal doping and up to several hundred degrees Kelvin¹. Though it is unlikely that all of the vast PG region is related to superconductivity (SC), there is compelling experimental evidence of anomalously strong SC fluctuations within PG^{2,3}. In particular, in the lightly doped cuprates, the SC fluctuation regime can be several times the SC transition temperature T_c . Here we examine the possibility that the enhanced SC fluctuations are a consequence of *stripes* – an intrinsic electronic inhomogeneity common to cuprates^{4–6}. By evaluating the strengths of the diamagnetic response and the Nernst effect within the striped SC scenario, we find results that are qualitatively consistent with the experimental observations³. Further, we make a prediction for anisotropic thermopower in detwinned samples that can be used to accurately test the proposed scenario.

There are two phenomena that have particularly high sensitivity to the presence of SC, even local or fluctuating one: the diamagnetic response and the Nernst effect. The diamagnetic part of field-induced magnetization can reveal the presence of SC inclusions, as they expel magnetic field, even if they are surrounded by completely non-SC (metallic or insulating) environment. The Nernst effect is a thermal analog of the conventional Hall effect – the transverse voltage generation driven by the heat current in the presence of a magnetic field. The Nernst effect in metals is typically very weak; however, in the presence of superconductivity it is greatly enhanced due to the thermal drift of SC vortices, which generates voltage via the Josephson relationship. In cuprates, the quasiparticle (qp) contribution may not be negligible⁷; yet, since the qp and the vortex contributions have different temperature dependences, and often even different signs, it is possible to disentangle the SC and qp contributions, even in the SC fluctuation regime.

The strong positive correlation between the Nernst effect and the diamagnetism measurements makes a compelling case for existence of SC fluctuations up to temperatures exceeding T_c by up to 50% near optimal doping and several times T_c deep in the underdoped La- and Bi-families of cuprates³. The very broad SC fluctuation regime defies explanation within the Gaussian

fluctuations approach⁸, which prompted the conjecture that instead of a soup of translationally invariant fluctuations, the SC response above T_c is governed by the quasi-static SC inclusions – “blobs”⁵. These blobs can preserve superconductivity – locally – up to temperatures T_c^* significantly higher than the T_c , at which the SC phase-locking occurs⁹. Below T_c^* , the nucleation of SC regions is also expected to reduce in-plane resistivity. Some experimental evidence for this reduction below an intermediate temperature scale, sometimes referred to as T_2^* (to distinguish from scale T^* that marks onset of antiferromagnetic fluctuations), indeed exists¹⁰ (Fig. 1).

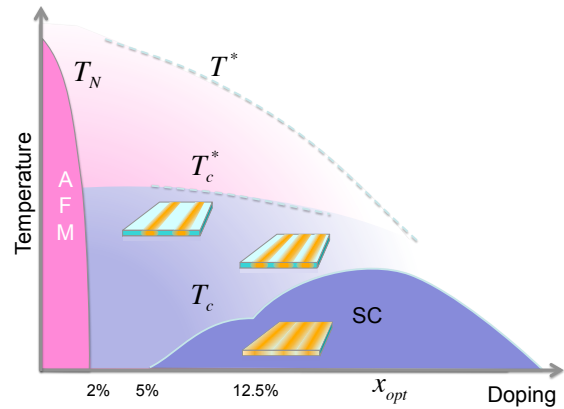


FIG. 1: Schematic phase diagram. Solid lines denote phase transitions into antiferromagnetic (AFM) and SC phases; dashed lines may either be phase transitions or crossovers, with T^* denoting the onset temperature of AFM fluctuations. The scale T_c^* corresponds to the considered here onset of local striped SC without global phase coherence.

Strongly inhomogeneous superconductivity may be caused by structural or chemical disorder. However, there is ample evidence for *intrinsic* spin/charge stripe inhomogeneity across all classes of hole-doped cuprates^{11–13}. The separation ℓ between stripes in the underdoped regime is controlled by doping x , $\ell \approx (2x)^{-1}$. Here we examine the possibility that SC follows the stripe pattern as well (Fig. 1), which is supported by the recent experiments¹⁴. Structural stripe fluctuations do not invalidate this picture, as long as their timescale is slower

than the characteristic time associated with superconductivity, $\sim \hbar/T_c$. Similar to the random blob scenario³, the global SC transition at T_c is associated with the phase-locking of the SC order parameter between the stripes, while *local* SC can persist up to the local mean-field transition temperature T_c^* . At low doping (below $\sim 12\%$), the stripes are well defined¹³ and thus superconductivity is strongly anisotropic. At higher doping, the overlap between stripes becomes significant, leading to a nearly uniform SC below T_c . Yet, in the interval of temperatures $T_c < T < T_c^*$, due to the destruction of SC in the inter-stripe regions, the striped nature of SC can become apparent even near optimal doping. This temperature interval is the most promising for detecting the presence of SC stripes.

Using the connection with the optimally doped uniform superconductor, we approximately identify the SC parameters (e.g., correlation length ξ and penetration depth λ_{ab}) of the stripe interior with the bulk parameters at the optimal doping. We also take the cross section of the superconducting stripes to be defined by the SC correlation lengths, $\xi_{ab} \times \xi_c$. In the direction along the stripes the correlation length is ξ_{ab} (Fig. 2A). These *intra-stripe* parameters change little through T_c below optimal doping.

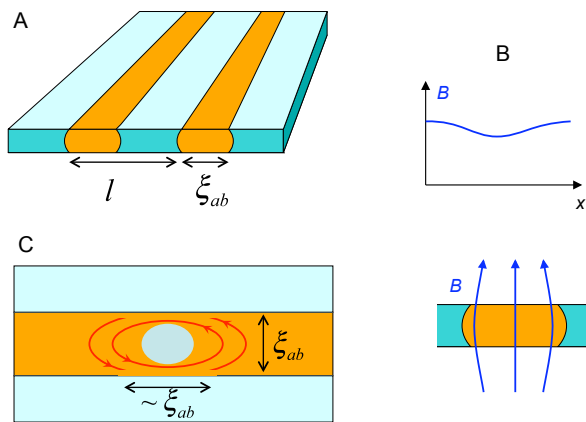


FIG. 2: (A) Schematic of a striped SC below optimal doping and above T_c . Orange regions are locally superconducting. (B) Weak expulsion of external magnetic field from the interior of the stripe due to the Meissner effect. (C) Vortex penetration into the SC stripe, red arrows denote diamagnetic (screening) currents.

Diamagnetism. Within our model, when superconducting stripes are exposed to magnetic field $H||\hat{z}$, the diamagnetic surface currents act to partially expel the field, as long as the field is less than the second critical field at optimal doping $H_{c2}^0(T)$ (Fig. 2B). The relevant penetration depth is $\lambda_{ab}(T)$ at optimal doping, whose

zero-temperature value in cuprates is about 200 nm^{15} . Since the in-plane width of the stripe is much less than the penetration depth, $\xi_{ab} \ll \lambda_{ab}$, the fraction of the flux expelled from the interior of the stripe is $(\xi_{ab}/\lambda_{ab})^2$. Averaging the diamagnetic response over SC and non-SC regions of space leads to an additional factor ξ_{ab}/l . Therefore, the result for the SC stripe-induced diamagnetic contribution to susceptibility above T_c is

$$\chi = \frac{\mu_0 M}{B} \sim -\frac{2\xi_{ab}^3(T)}{\lambda_{ab}^2(T)a} x, \quad (1)$$

where $\xi_{ab}(T)$ and λ_{ab} are functions of temperature, taken at optimal doping. The experimentally observed diamagnetic response in cuprates above T_c obeys the following pattern, independent of particular material¹⁶: $M \propto -B$ at small field, followed by a peak in $-M(B_p)$ at a temperature and doping dependent magnetic field $B_p(x, T)$, with the consequent disappearance of the diamagnetism at the high field $B_h(T)$. Within the scenario described here, $B_h(T)$ corresponds to the destruction of SC on the stripes. Therefore, we expect this field to be doping independent. This indeed appears to be true¹⁶; e.g. for temperatures below T_c^{opt} , B_h is about 40 T for Bi-2201, 70 T for Bi-2212, and 60 T for La-214. These values remain approximately constant from optimal to underdoped samples, while T_c changes by factor 2-3. At low applied fields, the measured linear susceptibility within a given family of compounds increases with doping¹⁶. This behavior, as well as the absolute magnitude, is qualitatively consistent with our estimate in Eq. (1).

Nernst effect. When a sample is subjected to a magnetic field $B||\hat{z}$ and an in-plane temperature gradient, e.g., $\nabla T||\hat{x}$, a transverse electric field E_y is induced. The Nernst signal is defined as $N(B, T) = E_y/(\nabla_x T)$ in the absence of any electrical currents. In general, there are both normal (qp) and superconducting contributions to the Nernst signal. The qp contribution can be either positive or negative, while the superconducting contribution is always positive within the given sign convention. The SC Nernst contribution has a simple interpretation in terms of thermally driven vortex motion¹⁷. Within our model of the striped superconductor above T_c , the vortices are defined only while they tunnel across the superconducting regions. Since the vortex core size is about the same as the width of the SC stripe, ξ_{ab} , during the vortex tunneling nearly whole cross section of the SC stripe becomes normal (Fig. 2C). As the amplitude of the superconducting order parameter vanishes, the SC phase can wind by $\pm 2\pi$, leading, according to the Josephson relationship, to a voltage pulse between the ends of the SC stripe. This *phase-slip* dynamics has been studied as the mechanism of electrical resistivity of thin superconducting wires¹⁸. In the case of a current-biased wire, the activation barrier for the phase slips, which generate positive voltage pulses, is lower than for the anti-phase slips. Upon time averaging, this leads to positive DC resistivity.

In the Nernst measurement, there is no applied cur-

rent; instead, the symmetry between vortex and anti-vortex tunneling across the SC stripes is broken by the external magnetic field. The vortices with magnetic moment m aligned with the external magnetic field have lower energy than anti-vortices, which carry moment $-m$. Thus, the activation barrier for a vortex/antivortex crossing a thin superconducting wire is $U_{v/av} = U_0 \mp mB$. The SC condensation energy within the region quenched by the vortex core is $U_0 \approx (1/\mu_0)B_c^2\xi_{ab}^2\xi_c$, with the thermodynamic critical field $B_c \approx \phi_0/(\lambda_{ab}\xi_{ab})$ and $\phi_0 = h/(2e)$ the flux quantum. The thermodynamic critical field is related to the second critical field¹⁹, $B_c \approx B_{c2}\xi_{av}/\lambda_{ab}$. The magnitude of the vortex/antivortex magnetic moment m can be estimated by noticing that the magnetization density near the vortex core scales as $(1/\mu_0)\phi_0/\lambda_{ab}^2$ and thus the total magnetic moment of a vortex confined to a SC wire of width ξ_{ab} and thickness ξ_c is about $m \sim (1/\mu_0)\phi_0\xi_{ab}^2\xi_c/\lambda_{ab}^2$. Therefore, for the tunneling energy barrier we obtain $U_{v/av} = U_0(1 \pm B/B)$, with $B \sim \phi_0/\xi_{ab}^2 \approx B_{c2}$, the second critical field.

Let us first assume that the stripes are perpendicular to the temperature gradient. Then, the temperature differential across the superconducting stripe is $\Delta T \approx |\nabla T|\xi_{ab}$. The activated tunneling rate for either vortices or antivortices is $\Gamma = \Gamma_0 e^{-U/T}$, where the prefactor can be estimated as $\Gamma_0 \sim T_c^*$ at temperatures below but not very near T_c^* . For the tunneling approach to apply, the barrier height has to be much larger than the temperature. Combining the vortex and antivortex tunneling contributions over the elementary stripe segments of length ξ_{ab} , and using the Josephson relationship, for the average electric field along the stripe we find,

$$N = \frac{E_y}{\nabla_x T} \sim \Gamma_0 \phi_0 e^{-\frac{U_0}{T}} \frac{U_0}{T^2} \left(\text{sh} \frac{U_0 B}{TB_{c2}} - \frac{B}{B_{c2}} \text{ch} \frac{U_0 B}{TB_{c2}} \right). \quad (2)$$

For small magnetic fields, $B < B_{c2}T/U_0$, the dependence is linear

$$\nu = \frac{E_y}{H \nabla_x T} \sim \Gamma_0 \phi_0 \frac{U_0^2}{T^3 H_{c2}} \exp -\frac{U_0}{T} \quad (3)$$

$$\sim \frac{k_B}{e H_{c2}} \left(\frac{U_0}{T} \right)^2 \exp -\frac{U_0}{T}. \quad (4)$$

For a typical value of $B_{c2} \sim 100$ T, we find that the first factor in the product is about 10^{-6} V/(K T), while the rest of the expression is very strongly dependent on the actual value of U_0/T . For instance, if $U_0/T = 5$, we find $\nu \sim 10^{-7}$ V/(KT).

For $U_0/T \gg 1$, at magnetic fields larger than $B_{c2}T/U_0$, from Eq. (2), the Nernst signal should increase non-linearly, reaching the U_0 -independent value $N_{max} \sim 0.2k_B/e \sim 20 \mu\text{V}/\text{K}$ below B_{c2} and then drop rapidly to zero at B_{c2} . Several theoretical curves for the Nernst signal at different temperatures are presented in Fig. 3.

For comparison with the experiment, we focus on the Bi and La families of cuprates known to have strong high-temperature SC fluctuations³. Overall, the experimentally observed behavior of the Nernst signal closely tracks

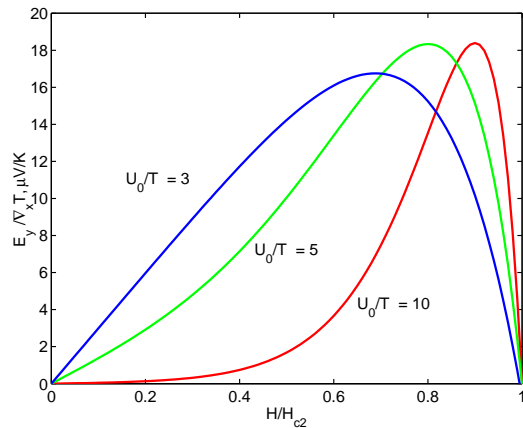


FIG. 3: Theoretical prediction of the Nernst signal based on the expression of Eq. (2) for several values of the ratio of the zero-field vortex tunneling barrier to temperature, U_0/T .

the features of diamagnetic response already described above. Namely, $N(B)$ has a pronounced dome-like shape, with the signal concentrated within an interval of magnetic fields that does not significantly depend on the doping. This is naturally consistent with the striped SC scenario, according to which the doping controls separation between the stripes but not their internal SC properties. Moreover, at low temperatures and small magnetic fields, a non-linear dependence $N(B)$ is observed, as is expected from Eq. (2). We can also roughly estimate the absolute magnitude of the Nernst effect. The main uncertainty is the value of U_0 since it appears in the exponent. Given the known optimal-doping properties of the cuprates, we estimate it to be below 500 K at zero temperature. For this rough value of the barrier, the theoretical amplitude of the Nernst signal is within the order of magnitude of the experimental observations.

Let us now consider the more general situation when the angle θ between the stripes and the direction of the applied thermal gradient (\hat{x}) is arbitrary. The temperature differential across the SC stripe that drives the vortex current will be reduced by the factor of $\sin \theta$. However, the length of stripe available for vortex tunneling will increase proportionately, as $\Delta \ell = \Delta y / \sin \theta$. We therefore conclude that the transverse electric field E_y is independent of the stripe orientation. This remains true even if stripes meander, as long as there are stripes connecting the two sides of the sample.

A direct consequence of the striped SC scenario for the Nernst effect is that in the samples where stripes run predominantly in one direction, there should be anisotropic SC contribution to thermopower that is odd in magnetic field. The electric field generated by the phase slips is aligned with the stripes; therefore, if stripes are not orthogonal to $\nabla_x T$, in addition to the transverse field E_y there should also be a *longitudinal* electric field

$$E_x = E_y \cot \theta. \quad (5)$$

The divergence of E_x for $\theta = (0, \pi)$ is clearly an artifact of our approximations, e.g., in treating the thermal gradient as constant throughout the sample. By symmetry, we expect that the vortex contribution to E_x at $\theta = (0, \pi)$ should be zero. For intermediate angles, our scenario predicts the B -dependent thermopower E_x comparable in magnitude to the Nernst electric field E_y . This prediction should be possible to test in the detwinned samples.

We now comment on other experimental implications of the striped SC scenario. The inhomogeneous superfluid density due to stripes will have signatures in the AC conductivity and in the penetration depth. Below T_c , at low doping, the superfluid stiffness is expected to be larger in the direction along the stripes (scaling as x), and smaller perpendicular to the stripes (scaling as $e^{-1/x}$). This anisotropy will lead to redistribution of the spectral weight of the real part of conductivity between the delta-function peak at zero frequency and the finite frequencies²⁰, when measured perpendicular to the stripes. This is indeed observed experimentally²¹. Inhomogeneous stripe-like superfluid density distribution can also lead to observable *in-plane* Josephson plasma resonance, in analogy to the more familiar *c-axis* plasma resonance²². Through T_c , the global phase coherence is

lost, however, the in-plane AC conductivity is expected to change gradually, with the SC signatures disappearing when the excitation frequency falls below the characteristic “phase slip” frequency of SC fluctuations²³.

In the preceding discussion the role of stripes was limited to providing the template for SC. It would be important to know if the presence of stripes *promotes* SC. An insight into this question could be obtained by correlating the high-temperature onset of incommensurate neutron scattering with the signatures of SC fluctuations. In this regard, it is suggestive that the highest onset temperature for the Nernst and diamagnetism in La-214 is at 12%³, precisely where the stripes are the most robust.

Acknowledgments: We acknowledge useful discussions with D. Podolsky and C. Kallin, and thank Aspen Center for Physics, where this work was initiated, for hospitality. The work of IM was carried out under the auspices of the National Nuclear Security Administration of the U.S. Department of Energy at Los Alamos National Laboratory under Contract No. DE-AC52-06NA25396 and supported by the LANL/LDRD Program. CP acknowledges financial support from MEXT-CT-2006-039047, EURYI and the National Research Foundation, Singapore.

-
- ¹ T. Timusk and B. Statt, Rep. Prog. Phys. **62**, 61 (1999).
² J. Corson et al, Nature **398**, 221 (1999).
³ Yayu Wang, Lu Li, N. P. Ong, Phys. Rev. B **73**, 024510 (2006).
⁴ J. Zaanen and O. Gunnarsson, Phys. Rev. B **40**, 7391 (1989).
⁵ J. M. Tranquada, B. J. Sternlieb, J. D. Axe, Y. Nakamura, and S. Uchida, Nature **375**, 561 (1995).
⁶ E. Berg, E. Fradkin, S. A. Kivelson, J. M. Tranquada, New Journal of Physics **11**, 115004 (2009).
⁷ R. Daou et al, Nature **463**, 519 (2010).
⁸ S. Ullah and A. T. Dorsey, Phys. Rev. B **44**, 262 (1991); I. Ussishkin, S. L. Sondhi, David A. Huse, Phys. Rev. Lett. **89**, 287001 (2002); K. Michaeli and A. M. Finkel’stein, Europhys. Lett. **86**, 27007 (2009).
⁹ J. M. Kosterlitz and D. J. Thouless, J. Phys. C: Solid State **6**, 1181 (1973).
¹⁰ J. L. Tallon and J. W. Loram, Physica C **349**, 53 (2001).
¹¹ Y. Ando, K. Segawa, S. Komiya, and A. Lavrov, Phys. Rev. Lett. **88**, 137005 (2002).
¹² Fujita et al, Phys. Rev. B **70**, 104517 (2004).
¹³ C. Howald, H. Eisaki, N. Kaneko, and A. Kapitulnik, Proc. Natl. Acad. Sci. U.S.A. **100**, 9705 (2003); Y. Kohsaka et al, Science **315**, 1380 (2007).
¹⁴ Q. Li, M. Hcker, G. D. Gu, A. M. Tsvelik, and J. M. Tranquada, Phys. Rev. Lett. **99**, 067001 (2007); ; K.-Y. Yang et al, New Journal of Physics **11**, 055053 (2009).
¹⁵ J. Tallon et al, Phys. Rev. B **68**, 180501(R) (2003).
¹⁶ L. Li et al, arXiv:0906.1823v3.
¹⁷ D. Podolsky, S. Raghu, and A. Vishwanath, Phys. Rev. Lett. **99**, 117004 (2007).
¹⁸ J. S. Langer and V. Ambegaokar, Phys. Rev. **164**, 498 (1967); D. E. McCumber and B. I. Halperin, Phys. Rev. B **1**, 1054 (1970).
¹⁹ P. G. de Gennes, *Superconductivity of metals and alloys* (W. A. Benjamin, Inc., New York - Amsterdam, 1966).
²⁰ S. Barabash, D. Stroud, and I.-J. Hwang Phys. Rev. B **61**, R14924 (2000).
²¹ J. Orenstein, arXiv:cond-mat/0201049v1; J. Orenstein, in *Handbook of High-Temperature Superconductivity*, J.R. Schrieffer and J.S. Brooks, eds. (Springer, 2007), p. 299.
²² M. Tachiki, S. Koyama, and S. Takahashi, Phys. Rev. B **50**, 7065 (1994); L. N. Bulaevskii, M. P. Maley, and M. Tachiki, Phys. Rev. Lett. **74**, 801 (1995).
²³ A. E. Koshelev, Phys. Rev. Lett. **77**, 3901 (1996).